Dietary strategies of Pleistocene *Pongo* sp. and *Homo erectus* on Java (Indonesia)

Jülide Kubat[1,2,3*], Alessia Nava[4,5*], Luca Bondioli[6,7], M. Christopher Dean[8], Clément Zanolli[9], Nicolas Bourgon[10], Anne-Marie Bacon[3], Fabrice Demeter[11,12], Beatrice Peripoli[7], Richard Albert[1,13], Tina Lüdecke[14,15], Christine Hertler[2,16], Patrick Mahoney[4], Ottmar Kullmer[2,17], Friedemann Schrenk[2,17], Wolfgang Müller[1,13,18*]

[1]Frankfurt Isotope and Element Research Center (FIERCE), Goethe University Frankfurt, Frankfurt am Main, Germany. [2]Department of Palaeoanthropology, Senckenberg Research Institute and Natural History Museum Frankfurt, Frankfurt am Main, Germany. [3]Université Paris Cité, CNRS, BABEL, 75012 Paris, France. [4]Skeletal Biology Research Centre, School of Anthropology and Conservation, University of Kent, Canterbury, UK. [5]DANTE Diet and ANcientTEchnology Laboratory – Department of Oral and Maxillo Facial Sciences, Sapienza University of Rome, Rome, Italy. [6]Bioarchaeology Service, Museum of Civilizations, Rome, Italy. [7]Department of Cultural Heritage, University of Padova, Italy. [8]Department of Earth Sciences Natural History Museum, London, UK. [9]Univ. Bordeaux, CNRS, MCC, PACEA, UMR 5199, 33600 Pessac, France. [10]Department of Human Evolution, Max Planck Institute for Evolutionary Anthropology, 04103 Leipzig, Germany. [11]Lundbeck Foundation GeoGenetics Centre, Øster Voldgade 5-7, 1350 Copenhagen, Denmark. [12]Musée de l'Homme, HNS, UMR 7206, 17 Place du Trocadéro, 75116 Paris, France. [13]Institute of Geosciences, Goethe University Frankfurt, Frankfurt am Main, Germany. [14]Emmy Noether Group for Hominin Meat Consumption, Max Planck Institute for Chemistry, 55128 Mainz, Germany. [15]Senckenberg Biodiversity and Climate Research Centre, 60325 Frankfurt, Germany. [16]ROCEEH Research Centre, Heidelberg Academy of Sciences and Humanities, Karlstrasse 4, 69117 Heidelberg, Germany.[17]Department of Paleobiology and Environment, Institute of Ecology, Evolution, and Diversity, Goethe University Frankfurt, Frankfurt am Main, Germany. [18]Senckenberg Research Institute and Natural History Museum Frankfurt, Frankfurt am Main, Germany.

*Corresponding authors: J. K. juelide.kubat@gmail.com, A. N. alessianava@gmail.com, W. M. w.muller@em.uni-frankfurt.de

During the Early to Middle Pleistocene, Java was inhabited by a high variety of hominid taxa with hitherto unclear seasonal dietary strategies. We undertook the first geochemical

analyses of *Pongo* sp., *Homo erectus* and other mammalian Pleistocene teeth from Sangiran. We reconstructed past dietary strategies at sub-weekly resolution and inferred seasonal ecological patterns. Histologically-controlled spatially-resolved elemental analyses by laser-based plasma mass spectrometry (LA-ICPMS) confirmed the preservation of authentic biogenic signals despite the effect of spatially-restricted diagenetic overprint. The Sr/Ca record of faunal remains is in line with expected trophic positions, contextualizing fossil hominid diet. *Pongo* sp. displays marked seasonal cycles with ~3-month-long strongly elevated Sr/Ca peaks, reflecting contrasting plant food consumption presumably during the monsoon season, while lower Sr/Ca ratios suggest different food availability during the dry season. In contrast, omnivorous *Homo erectus* shows low and less accentuated intra-annual Sr/Ca variability compared to *Pongo* sp., with $\delta^{13}C$ data of one individual indicating dietary adaptation from C_3 to C_4 plants through its lifetime. We infer that *Homo erectus* was likely affected by seasonal fluctuations of food availability, but to a lesser degree than *Pongo* sp. We suggest that *Homo erectus* maintained its nutritional demands more independent from seasonal fluctuations by exploiting the regional diversity of food resources.

The Pleistocene hominid fossil record from the Sangiran Dome in Central Java, Indonesia, is one of the largest palaeoanthropological collections in Southeast Asia, evidencing an Early Pleistocene expansion of *Homo erectus* onto the Sunda Shelf[1–4]. The high morphodimensional variability of Indonesian hominid specimens led in the past to the attribution of the fossils to a variety of taxa such as *Homo erectus*, *Meganthropus palaeojavanicus, Pithecanthropus dubius* or *Pongo* sp. fuelled taxonomic debates[1,5–9]. Recently, a high level of Javanese hominid palaeodiversity was revealed, which confirmed the taxonomic validity of the genus *Meganthropus*, a taxon that coexisted with *H. erectus* and *Pongo*[10]. Although dental macrowear and enamel thickness broadly reflect different dietary adaptations among these hominids[10], little is known about their detailed ecological niches and their inter- and intraspecies competition and interaction.

Previous geochemical analyses of tooth enamel provided insights into palaeoenvironment, palaeodiet and life history of extinct hominins such as *Australopithecus*[11,12], *Paranthropus*[11] and Neanderthals[13,14]. Tooth enamel – contrary to bone and dentine – is less prone to post-mortem diagenetic alteration due to its highly mineralized nature[15,16]. Moreover, it mineralizes sequentially in utero and during infancy to early adolescence and, once fully mineralized, remains compositionally and structurally stable during life. Consequently, enamel captures and preserves environmental and dietary changes that occur during the enamel mineralization phases in an individual's life[17–20]. Elemental and isotopic analysis by laser-ablation inductively-coupled-plasma mass spectrometry (LA-ICPMS) across the incremental structures of sequentially secreted enamel provides a temporally and spatially highly-resolved record of an individual's childhood. Such data allow the interpretation of diet, health, growth rates, weaning, and mobility as well as changes of the environmental setting on a seasonal to weekly scale[13,14,21–23]. Trace element ratios strontium/calcium (Sr/Ca) and barium/calcium (Ba/Ca) in dental enamel can record dietary signals due to the biopurification of Ca in trophic chains[24–26]. The higher the trophic level, the less [Sr] and [Ba] relative to [Ca] are incorporated into enamel, resulting in higher values of trace element ratios in herbivore enamel than that of omnivores or carnivores[11,24,27], though additional factors such as soil ingestion play a role[28].

To assess dietary and life history signals in Pleistocene *H. erectus* and *Pongo* sp. from the Sangiran Dome, we explored Sr/Ca and Ba/Ca ratios and other trace element signals at high spatial/time-resolution in dental enamel of premolars and molars from these taxa. For comparison and as trophic level reference, we utilized isolated premolars and molars of mammalian specimens belonging to different families (Felidae, Rhinocerotidae, Suidae, Cervidae, Hippopotamidae; Table 1) from the Sangiran fossil assemblage presumably co-existing with various hominid taxa such as *H. erectus*, *Meganthropus* and *Pongo*[10,29,30].

All specimens were recovered from either the Early Pleistocene Sangiran Formation, or from the later Early to initial Middle Pleistocene Bapang Formation, as both are fossiliferous, and contain sequential faunal assemblages and taxa[4,31,32]. However, the exact stratigraphic allocation of all specimens is not documented[2,32]. The geological age of the specimens ranges between 1.4 to 1.0 Ma and 1.0 to 0.7 Ma for specimens from the Sangiran and Bapang Formations, respectively[4].

We focused our study on Sr/Ca (and to a lesser extent Ba/Ca) ratios as (relative) trophic level proxies, including an assessment of how well biogenic geochemical information is preserved in Pleistocene bioapatite from (sub)tropical contexts by utilizing elements Mn, Al, Y, Ce, U as tracers of post-mortem alteration [14,27,28,33-37].Previous stable isotope analyses of *H. erectus* bone samples from Sangiran were not successful in obtaining palaeoecological signals due to diagenetic alteration of bone tissue[38]. Here we include carbon ($\delta^{13}C$) and oxygen ($\delta^{18}O$) isotope analyses of dental enamel of one *H. erectus* permanent premolar (S7-37) in order to contextualize our elemental results and obtain additional dietary/environmental information.

Results

In Table 2 we report Retzius periodicity (RP), laser track length and the corresponding time-span for the analyzed samples. The RP of *Pongo* sp. SMF-8864 was obtained through direct counts of cross striations between two adjacent Retzius lines. The RP of *Homo erectus* SMF-8865, given the section thickness necessary for chemical analyses and the presence of some accentuated markings, was calculated as the distance between adjacent Retzius lines divided by local daily secretion rate (DSR); the latter directly measured in areas of the section where the cross striations were clearly visible. For *Homo erectus* S7-37 P^4, we report the RP calculated in[18] for the S7-37 M^1 belonging to the same individual.

Elemental signals were retrieved within enamel close to the enamel-dentine-junction (EDJ; <100 µm) because it is where environmental signals are best captured topographically during secretion and elemental overprint during enamel maturation has the least effect[14,22,39–41]. For assessing post-mortem diagenetic overprint, scatterplots of [Sr] or [Ba] vs. [Mn] or [U] at EDJ profiles of representative samples of each trophic level were generated (Fig. 1 and Supplementary Fig. 1). All cases show clearly positive correlations between trace elements and diagenesis-indicating element concentrations. Even though multi-stage diagenetic histories may be indicated by different trajectories (Fig. 1), uptake of Sr and Ba with increasing geochemical alteration is evident, which implies that the best approximations of initial biogenic [Sr] or [Ba] (or expressed as Sr/Ca, Ba/Ca

ratios) can be found at lowest [Mn] or [U]. These plots also reveal that [Sr] increases by a maximum of ~180%, while [Ba] is characterized by a threefold to tenfold increases, confirming the higher susceptibility of Ba to post-mortem overprint. Repeat profiles at the EDJs of both tooth aspects and along prism directions indicate greater consistency between corresponding Sr/Ca profiles, relative to those of Ba/Ca (Supplementary Figs. 2-6). Using [Mn] and [U] thresholds of 400 and 1 ppm, respectively, to screen Sr/Ca and Ba/Ca trophic level signals, revealed expected patterns for trophic groups for Sr/Ca, but more ambiguous ones for Ba/Ca (Fig. 2; Supplementary Fig. 7). As a result, we focus more on Sr/Ca results but also note that Ba/Ca can indicate reliable results in case of well-preserved samples (e. g., *Pongo* SMF-8864, see below).

The Sr/Ca ratio boxplots of faunal and hominid specimens (Fig. 2) show carnivorous Felidae with the lowest Sr/Ca ratio in the faunal assemblage (~$8.4*10^{-4}$), following the expected trophic level trend towards lower Sr/Ca ratios relative to omnivores ($1.1*10^{-3}$; represented by Suidae) and different herbivore groups ($1.6*10^{-3}$ – $4.0*10^{-3}$). Rhinocerotidae exhibit a Sr/Ca level ~2 times higher than all other herbivores and a broad Sr/Ca variability. The three *H. erectus* dental specimens yield Sr/Ca ratios between those of the Felidae and Suidae. The *Pongo* sp. specimen SMF-8864 shows the largest variation in Sr/Ca distribution among all taxa and has a large number of distributional outliers toward higher Sr/Ca values (Fig. 2). Its median value fits well within the Hippopotamidae and Cervidae central distributions. The peculiar distribution of Sr/Ca values in *Pongo* sp. SMF-8864 is the result of distinct biogenic Sr/Ca peaks throughout the life of this individual and not of diagenetic origin, as shown by the diagenetic indicators concentration values (see below).

The elemental ratio profiles in hominid tooth enamel were aligned with the individual odontochronologies (see Figs. 3 and 4; Supplementary Figs. 2-6) on both lingual and buccal aspects (except for S7-37 P^4 where only the buccal aspect was available for analysis) to derive Sr/Ca (and Ba/Ca) variation vs. time (secretion-days). Only for S7-37 P^4 the life time referred to birth is available following[42] but not for molars with uncertain position such as S7-13, SMF-8864, SMF-8865, although we tentatively attribute molar positions based on some diagnostic morphological features described in the Supplementary Information and corresponding chemical signals. Figure 3a shows the Sr/Ca and Ba/Ca EDJ profiles together with diagenesis-indicating [U] and [Mn] against time for the 1073

days (~2 years and 11 months) of the buccal aspect of the *Pongo* sp. SMF-8864 molar. EDJ (Fig. 3a) and corresponding prisms (P; Fig. 3b and Supplementary Fig. 4) Sr/Ca profiles for the buccal enamel show good agreement but invariably lower Sr/Ca values towards outer enamel along the prisms (Fig. 3b), as expected by the effect of maturation overprint[22]. The buccal and lingual Sr/Ca EDJ profiles of *Pongo* sp. SMF-8864 are compared in Fig. 3c to assess the reproducibility of in-vivo elemental signals. The time span covered by the lingual aspect is 1339 days (~3 years and 8 months; Fig. 3c). Generally, [Mn] and [U] on both sides of the crown are at detection limit, with [U] rising to a maximum of ~2 ppm for the final ~100 days of thin cervical enamel. Neither Sr/Ca nor Ba/Ca ratios are strongly affected by these minor [U] increases confirming the biogenic nature of the signal; yet we note that some smaller Ba/Ca-peaks co-occur with minor U-peaks (e.g., ~930 days; Fig. 3a).

The consistency of the chronologies is attested by the high correspondence of the Sr/Ca signals between the two EDJ and prisms profiles. *Pongo* sp. SMF-8864 exhibits stark intra-tooth variability with three distinct peaks characterized by up to sixfold Sr/Ca and ~eightfold Ba/Ca increases. This sixfold Sr/Ca change for the first peak ($1.8*10^{-3}$ to $10.7*10^{-3}$) decreases for the second and third peaks to threefold and twofold values, respectively. The influence of the Sr/Ca attenuation along prisms towards outer enamel[22] is discernible but partly compensated for in e. g., prism 3 by the strong biogenic signal (Fig. 3b). On the buccal side, three hypoplastic defects and four accentuated lines (AL) are present (Fig. 3c), yet these non-specific growth disturbances[42] are not coincident with the Sr/Ca (or Ba/Ca) trends. The interval between the midpoints of two consecutive peaks on the buccal aspect approximates one year, namely 364 and 324 days between peaks 1–2 and peaks 2–3, respectively. The duration of these peaks is 95, 118 and 90 relative days for the first, second and third peak, respectively, approximating an overall duration of three months each.

The Sr/Ca-profiles of the three *H. erectus* samples display low [U] and [Mn] and thus acceptable preservation, apart from localized peaks indicating spatially-restricted diagenetic alteration (Fig. 4). Comparative elemental profiles for the lingual and buccal aspects of two *H. erectus* specimens presented in Supplementary Figures 2 and 3, illustrate that enamel of the same tooth may be variably preserved yet we utilized the better preserved domains. Limited inter-sample Sr/Ca-variation ranges between $0.7–1.4*10^{-3}$, while intra-profile Sr/Ca-variability is 20–30%. These *H. erectus* Sr/Ca-values

are thus always below those in *Pongo* sp. SMF-8864, which is even more pronounced for the intra-sample variability (20–30 vs. 200–600%). The temporal spacing between broad Sr/Ca troughs and/or peaks in all samples lies between 340–380 days, consistent with approximately annual cyclicity. As it is uncertain which of the apparent minor Sr/Ca fluctuations are indicative of variable food intake or minor cryptic diagenetic overprint, we refrain from attributing unwarranted importance to small-scale variability. Despite the uncertain molar position for *H. erectus* SMF-8865, the stability of the Sr/Ca ratio in the first 220 days of tooth formation suggests the absence of the breastfeeding signal[14,22]. Therefore, the tooth likely is not a first permanent molar which starts to form earlier in life.

We report sequentially-microsampled stable carbon and oxygen isotope compositions of enamel derived from S7-37 P^4 (n = 3; Fig. 5; Supplementary Table 1). The samples correspond to three distinct portions of the dental crown representing three partially overlapping life time moments. $\delta^{13}C$ values range from –4.9 to –2.4 ‰ (average = –3.9 ± 1.4 ‰ (1s)), suggesting a diet which ranged from a mixed C_3/C_4 plant consumption to dominated C_4 plant consumption (54 to 72 % C_4 fraction in the diet, calculated after[43]). $\delta^{18}O$ values remain stable with only very little variation between –6.7 and –5.9 ‰ (average = –6.3 ± 0.4 ‰).

Discussion

Hominid Retzius periodicity. Retzius periodicities of 7 to 9 days for our sample of *H. erectus* teeth are typical of these early humans. They are similar to the periodicities reported previously for *Homo erectus/ergaster* molars and premolars (7-8 and 9 days, respectively)[44], but this apparent tighter distribution of values differs from the wider range of periodicities between 6 to 12 days characteristic of larger samples of living humans[45]. An 8-day periodicity for the *Pongo* sp. lower molar SMF-8864 is slightly lower than the 9 to 12-day periodicity reported for fossil *Pongo* from Sumatra and mainland Asia[46] but lies within the range of values (8–11 days) reported for living *Pongo*[47].

Hominid trophic levels at Sangiran. Trophic levels portray the relative position of species in a food web and are important for ecosystem functioning[48]. Fossil teeth of Carnivora (Felidae), Perissodactyla (Rhinocerotidae), and Artiodactyla (Suidae, Cervidae, Hippopotamidae) from the Sangiran Dome with known trophic levels were used to establish an underlying relative trophic level framework for Sangiran. The ordering of fossil faunal taxa from Sangiran according to their enamel Sr/Ca ratios ($Sr/Ca_{carnivores} < Sr/Ca_{omnivores} < Sr/Ca_{herbivores}$) reflects trophic level differences that are in good agreement with their expected dietary habits (Fig. 2)[11,49], suggesting reliable trophic level determination based on enamel Sr/Ca.

The *Pongo* sp. lower molar SMF-8864 exhibits a high intra-tooth variability, caused by cyclical Sr/Ca peaks (Fig. 3) along the EDJ profile covering the whole range of other herbivorous specimens in this study. The average Sr/Ca ratios between the peaks is closer to the Sr/Ca ratio of herbivorous animals such as *Hexaprotodon* sp. and *Axis lydekkeri*[50–53]. The maximum Sr/Ca values for the first and second peaks are exceeding those of the rhinocerotids (for whom soil or dust ingestion might additionally lead to elevated Sr/Ca)[28]. The lowest Sr/Ca values in SMF-8864 overlap with those of suids and with the higher values of felids. This fits well with the known versatile diet of living orangutans, which includes fruits, flowers, bark, insects, eggs and occasionally meat[54,55]. The *H. erectus* lower molar SMF-8865 shows Sr/Ca ratios similar to *H. erectus* individuals S7-13 and S7-37. All *H. erectus* specimens in this study group with omnivorous (Suidae) and carnivorous (Felidae) mammals from Sangiran (Fig. 2), suggesting an omnivorous diet with a certain degree of meat consumption for *H. erectus* on Java.

Comparison of Sr/Ca patterns in *Homo erectus* and *Pongo* sp. The biogenic Sr/Ca peaks in *Pongo* sp. SMF-8864 occur nearly annually (Fig. 3). The Sr/Ca variation in *H. erectus* SMF-8865 also shows cyclical pattern: the duration of the cycle is approximately 345 days. *H. erectus* S7-13 shows a complete cycle of 347 days and a partial cycle of 148 days. The preserved portion of the crown ends before the end of the cycle. *H. erectus* S7-37 also shows two cycles with a duration of 375 relative days and 383 relative days. The second cycle is marked by two smaller Sr/Ca decreases

within the cycle. Uranium does not follow the annual cycle trend in any of the samples, thus suggesting negligible influence of diagenetic imprint (Fig. 4a-c). In summary, all *H. erectus* individuals demonstrate low-amplitude Sr/Ca cycles with a duration of approximately one year, whereas *Pongo* sp. SMF-8864 demonstrates two cycles with sharp peaks that last 3–4 months.

Diet of *Pongo* sp. reflects high seasonal food variability. The cyclical pattern of Sr/Ca and Ba/Ca peaks in *Pongo* sp. SMF-8864 with higher ratios occurring on an essentially annual basis gradually decreases within the ~3 years of life represented by the tooth (Fig. 3). This Sr/Ca and Ba/Ca peak height decrease towards the neck of the tooth may be explained by increased maturation overprint, which is inversely proportional to enamel thickness[22]. The repeatedly high Sr/Ca and Ba/Ca signals in this sample likely reflect annual periods with an increased intake of plant-based food resources, probably linked to a higher food availability during monsoonal periods and mast-fruiting events, with a variation of the peak heights also linked to different food intake[56]. Studies of palaeosols and the occurrence of palaeovertisols in the Sangiran Dome strongly suggest that Java was a monsoon region in the Early Pleistocene, with an annual dry season[3]. Monsoonal rain forest was likely the major vegetation type of Central Java during the Early Pleistocene[57-59].

A recent study suggested a causal relationship to a cyclical nursing pattern, which results in a cyclical increase of Ba concentrations in teeth (i.e., increased intake of mothers' milk)[60]. However, the synchronous up to sixfold increase in Sr/Ca and up to eightfold increase in Ba/Ca are unlikely to reflect a breastmilk signal because of depletion of breast milk Sr due to epithelial discrimination in mammary glands[14,22, 61,62].

Recent studies on cementum in *Pongo* revealed that regions of [Sr] enrichment and depletion relate to seasonal fluctuations in diet rather than cyclical breastfeeding[63,64]. Caloric intake in orangutans is 2-3 times greater during masting events[56], which are usually followed by periods of low fruit availability during dry periods, compensated in turn by burning fat reserves stored during mast-feeding[65]. Sr/Ca and Ba/Ca signals might also be enhanced during episodes of mast-feeding because of geophagic behaviour, i.e. the deliberate ingestion of soils enriched in trace elements,

which absorb toxins and tannins[64]. This behaviour was previously observed in orangutans[66]. Geophagy combined with the high availability of food resources during monsoonal seasons might be the reason for the elevated Sr/Ca and Ba/Ca peaks.

It has been shown that non-specific stress enamel markers (accentuated lines, ALs) can be correlated to variations in barium concentrations in dental tissues of primates[67]. In *Pongo* sp. SMF-8864, four ALs, occurring between the first and the second peaks (Fig. 3c), show a weak or absent correlation with elemental variations. However, the ALs' position outside of the peaks' regions provide possible evidence of seasonal effects, as they might reflect stress events occurring during the first identified dry season. Hypoplastic defects on the tooth crown as a further sign of physiological stress do not correlate with elemental variations too (Fig. 3c) and indicates more complex, still-to-define developmental deficiencies[14,42].

Orangutans have the slowest life histories of any non-human primates with the latest weaning age of any mammals at around 7 years, but with relatively low levels of nutrient transfer during breast-feeding[60,68,69,70]. Consequently, solid foods are supplemented in the infant's diet between 1 and 1.5 years of age, to compensate additional nutritional demands[60,69]. Infants can forage solid foods independently from the age of ~1.5 years, whilst the mother is not decreasing her lactation efforts[69]. Dry seasons with low food availability are compensated by extending weaning ages for infants leading to low growth and reproduction rates and solitary lifestyles[65,71-73].

Dietary strategy of *Homo erectus*. The three *H. erectus* specimens show distinct Sr/Ca cycles with a duration of approximately one year (Fig. 4). In contrast to the results from *Pongo* sp., the yearly Sr/Ca cycles in *H. erectus* are of low amplitude (20 - 30 %), which are much smaller than the seasonal changes observed in *Pongo* sp. SMF-8864. For *H. erectus*, these might reflect the consumption of specifically selected animal or plant resources, which were available in the regional context of a highly diverse ecosystem. Our $\delta^{13}C$ data show that the analyzed *H. erectus* individual consumed a mix of C_3 and C_4 biomass at the start of P^4 mineralization and then changed to a C_4-dominated diet in the later stages of P^4 mineralization (Fig. 5).

The small variation of the relatively low $\delta^{18}O$ values (Fig. 5) of the analyzed *H. erectus* indicates that the individual had access to a freshwater source during the whole time of P^4 tooth formation. Therefore, *H. erectus* might have exploited regionally available resources and consumed water and/or aquatic foods from e.g., rivers. Nearly 70 km east of Sangiran, at the site of Trinil where *H. erectus* was first discovered and described[74,75], it was suggested that members of this species likely consumed aquatic resources like shellfish, indicating a high level of food resilience[76]. In general, a high adaptive versatility is assumed for early members of the genus *Homo*[77]. In addition, dental microwear traits in Sangiran *H. erectus* teeth also confirm an opportunistic omnivorous dietary strategy[78,79].

Conclusions

The main outcome of the present study is the demonstration that both *Pongo* sp. and *H. erectus* at Sangiran had cyclical food resource availability with a yearly period. However, distinct differences in the chemical pattern point to dietary and life history differences of Pleistocene Southeast Asian *Pongo* sp. and *H. erectus*, both reacting to seasonal resource variations differently. While *Pongo* sp. consumed contrasting plant-based food resources during the wet (monsoonal) season presumably available in moonsonal rain forests, *H. erectus* was more versatile and exploited a broader range of high diversity food resources, possibly along riverine habitats as suggested by the near-uniform oxygen isotopic composition.

We demonstrate the effective use of histologically-controlled time-resolved LA-ICPMS elemental analyses of hominid dental fossils to retrieve biogenic signals at sub-weekly time resolution. Our results show the first time-resolved geochemical analyses on *Homo erectus* from the Sangiran Dome, which showcases the importance of geochemical analysis of fossil dental enamel of early humans to reconstruct past dietary behaviours and life histories in an evo-devo perspective.

Methods

Overall the methodologies employed here follow those in Nava et al. 2020[14] and Müller et al. 2019[22] and only a brief summary is given here below.

Enamel thin sections. Preparation, imaging and histological analysis of enamel thin sections[80,81] were carried out at the Museo delle Civiltà in Rome. Sectioning was performed using a Leica high precision diamond blade (Leica AG) and IsoMet low speed diamond blade microtome (Buehler Ltd). Sections were ground with Minimet 1000 Automatic Polishing Machine (Buehler Ltd) using silicon carbide grinding papers with two grits (1000 and 2500; Buehler Ltd). Sections were polished using a Minimet 1000 Automatic Polishing Machine (Buehler Ltd) with a micro-tissue damped with distilled water and diamond paste (Diamond DP-suspension M, Struers) containing 1 µm sized monocrystalline diamonds. Thickness of the faunal thin sections was 130–150 µm depending on the preservation and visibility of the enamel microstructure. The hominid section thickness varied between 250 and 400 µm, thus facilitating the geochemical analysis but ensuring sufficient readability of the enamel microstructures.

LA-ICPMS analyses. LA-ICPMS analyses were carried out at the Frankfurt Isotope and Element Research Centre (FIERCE), Goethe University (Frankfurt am Main). Histologically-controlled tracks were determined on the enamel micrographs with Photoshop (Adobe Inc.). Sampling included continuous laser ablation tracks in enamel <100µm parallel to the EDJ following the tooth growth direction[22].

The LA-ICPMS system includes an 193nm ArF excimer laser (RESOlution S-155; now Applied Spectra, Inc. (ASI), USA) coupled to a two-volume laser ablation cell (Laurin Technic, Australia)[22,82]. The laser ablation system is connected to an ICPMS Element XR™ (Thermo Fisher Scientific) using nylon6-tubing. Thin sections were ultrasonically cleaned with methanol and fixed in the sample holder together with a series of primary and secondary standards. The micrographs with pre-marked laser tracks were uploaded in GeoStar µGIS Software (Norris Scientific, Australia) and retraced

before LA-analyses. LA-ICPMS data acquisition was performed in continuous path mode due to the benefits of a two-volume LA cell with fast signal washout and constant signal response[22,82].

Prior to analysis, laser tracks were cleaned with a bigger spot size (40 µm), higher repetition rate (20 Hz) and scan speed (varying between 16.7-30 µm/s depending on the size of teeth) to remove surface residues, which could alter the results[83]. Analyses were carried out with a spot size of 18 µm, scan speed of 10 µm/s and a repetition rate of 15 Hz. The time signal obtained from the ICPMS can be directly transferred to distance along the LA tracks via the constant scan speed of the laser X-Y stage; no time delays of the X-Y stage exist at waypoints of composite tracks[22]. Between the LA system and the ICPMS, a signal smoothing device ("squid") was included[82].

The ICPMS (Element XR) detected the following isotopes from the ablated sample material (m/z):^{25}Mg, ^{27}Al, ^{43}Ca, ^{44}Ca, ^{66}Zn, ^{86}Sr, ^{88}Sr, ^{89}Y, ^{138}Ba, ^{140}Ce, ^{208}Pb, ^{238}U. For calibration purposes (following Longerich et al. 1996[84]), NIST612 as a primary external standard and ^{44}Ca as internal standard were used. In bioapatite, Ca is commonly used as an internal standard, which is set at 37%[22,85,86], but for elemental ratios no prior knowledge of the sample [Ca] is necessary. For NIST 612 the following preferred values (± 2SD (in %)) were used (from GeoREM website http://georem.mpch-mainz.gwdg.de): CaO: 11.9 ± 0.4%m/m; Zn: 38 ± 4, Sr: 78.4 ± 0.2, Y: 38 ± 2, Ba: 39.7 ± 0.4, Ce: 38.7 ± 0.4, Pb: 38.57 ± 0.2, U: 37.38 ± 0.08 µg/g.

Secondary standards with known concentrations and a matrix broadly similar to apatite (STDPx glasses) were analyzed to assess accuracy and precision: STDP3-150, STDP3-1500, STDP5 (Ca-P-(Si) glass standards)[87], KL2-G (basalt glass)[88], MAPS5 (phosphate pellet) and MACS3 (Microanalytical Carbonate Standard; United States Geological Survey USGS: preliminary Certificate of Analysis by Steve Wilson), both available as 'nano'pellets from D. Garbe-Schönberg[89,90]. MACS3 was used for Zn accuracy because no reported Zn values are available for the Ca-P-(Si) glass standard[22]. Comparisons between measured secondary standard concentrations and reported concentrations revealed that the most accurate results with the lowest average bias were produced using the combination of NIST612 with ^{44}Ca. Average relative biases of all three STDPx standards and MAPS5 were (in %): Al: -2.87 ± 3.26, Ca: 2.62 ± 1.72, Rb: 2.14 ± 20.47, Sr:

2.57 ± 4.98, Y: 5.85 ± 3.11, Ba: 0.68 ± 5.23, Ce: -1.31 ± 3.46, Pb: -2.88 ± 10.33, U: 2.80 ± 5.48 (average bias of all standards ± 1SD in %).

The compositional profiles displaying the concentration of elements relative to distance/days along the EDJ profile were smoothed with a locally weighted polynomial regression fit, with its associated standard error range (±2 SE) for each predicted value[91]. The software R (ver. 4.0.4; R-Core-Team, 2021) and the packages “lava”, “readxl”, “shape” and “tidyverse” were used for all statistical computations and generation of graphs.

Elemental data was matched with odontochronologies of the *H. erectus* and *Pongo* sp. Specimens by determining the chronology of each EDJ track after LA-ICPMS analysis (Supplementary Fig. 8), and directly assessing the enamel daily secretion rates (DSR). DSR i. e. the speed at which the ameloblast - the enamel forming cells - move towards the outer surface of the tooth is expressed in µm day^{-1} along the prisms[92,93], in the 100 µm region close to the EDJ. Carefully chosen histologically-defined (EDJ) profiles facilitate the correlation between odontochronological and geochemical signals at a very high time resolution (<1 week).

Isotopic ratio mass spectrometry (IRMS) analyses. Stable carbon and oxygen analyses of S7-37 (right P^4) were performed at the Goethe University-Senckenberg BiK-F Joint Stable Isotope Facility Frankfurt, Germany. 2.9 to 3.8 mg of enamel powder was retrieved for each sample with a hand-held diamond tip dental drill. To produce sufficient sample material, drill holes were expended perpendicular to the growth axis of the teeth.

To remove organic matter and potential diagenetic carbonate, enamel was pretreated with 2 % NaOCl solution for 24 hours followed by 1 M Ca-acetate acetic acid buffer solution for another 24 hours and thoroughly rinsed with deionized water. Typically, enamel pre-treatment resulted in ~60 % mass loss. Then, 950 to 1100 µg of pretreated enamel powder were reacted with 99% H3PO4 for 90 min at 70 °C in continuous flow mode using a Thermo Finnigan 253 mass spectrometer interfaced to a Thermo GasBench II. Analytical procedure followed the protocol of Spötl and Vennemann (2003)[94]. Final isotopic ratios are reported versus VPDB (Vienna Pee Dee Belemnite); overall analytical uncertainties are better than 0.3 ‰ for $\delta^{13}C$ and 0.05 for $\delta^{18}O$.

References

1. von Koenigswald, G. H. R. Fossil hominids from the Lower Pleistocene of Java. in *Rep. 18th Internat Geological Congress* 59–61 (1948).

2. Grine, F. E. & Franzen, J. L. Fossil hominid teeth from the Sangiran Dome (Java, Indonesia). *Cour. Forsch. Inst. Senckenberg* **171**, 75–103 (1994).

3. Bettis, E. A. *et al.* Way out of Africa: Early Pleistocene paleoenvironments inhabited by *Homo erectus* in Sangiran, Java. *J. Hum. Evol.* **56**, 11–24 (2009).

4. Matsu'ura, S. *et al.* Age control of the first appearance datum for Javanese *Homo erectus* in the Sangiran area. *Science* **367**, 210–214 (2020).

5. Weidenreich, F. Giant early man from Java and South China. *Anthropol. Pap. Am. Mus. Nat. Hist.* **40**, 1–134 (1945).

6. von Koenigswald, G. H. R. *Pithecanthropus*, *Meganthropus* and the Australopithecinae. *Nature* **173**, 795–797 (1954).

7. Franzen, J. L. What is "*Pithecanthropus dubius* Koenigswald, 1950"? In *Ancestors: The Hard Evidence* (ed Delson, E.) 221–226 (Alan R. Liss, Inc., New York, 1985).

8. Tyler, D. E. Sangiran 5, ("*Pithecanthropus dubius*"), *Homo erectus*, "*Meganthropus*," or *Pongo*? *Hum. Evol.* **18**, 229–241 (2003).

9. Tyler, D. E. An examination of the taxonomic status of the fragmentary mandible Sangiran 5, (*Pithecanthropus dubius*), *Homo erectus*, '*Meganthropus*', or *Pongo*? *Quat. Int.* **117**, 125–130 (2004).

10. Zanolli, C. *et al.* Evidence for increased hominid diversity in the Early to Middle Pleistocene of Indonesia. *Nat. Ecol. Evol.* **3**, 755–764 (2019).

11. Balter, V., Braga, J., Télouk, P. & Thackeray, J. F. Evidence for dietary change but not landscape use in South African early hominins. *Nature* **489**, 558–560 (2012).

12. Joannes-Boyau, R. *et al.* Elemental signatures of *Australopithecus africanus* teeth reveal seasonal dietary stress. *Nature* **572**, 112–115 (2019).

13. Smith, T. M. *et al.* Wintertime stress, nursing, and lead exposure in Neanderthal children. *Sci. Adv.* **4**, 9483–9514 (2018).

14. Nava, A. *et al.* Early life of Neanderthals. *Proc. Natl. Acad. Sci. USA* **117**, 28719–28726 (2020).

15. Hoppe, K. A., Koch, P. L. & Furutani, T. T. Assessing the preservation of biogenic strontium in fossil bones and tooth enamel. *Int. J. Osteoarchaeol.* **13**, 20–28 (2003).

16. Hinz, E. A. & Kohn, M. J. The effect of tissue structure and soil chemistry on trace element uptake in fossils. *Geochim. Cosmochim. Acta* **74**, 3213–3231 (2010).

17. Bromage, T. G., Hogg, R. T., Lacruz, R. S. & Hou, C. Primate enamel evinces long period biological timing and regulation of life history. *J. Theor. Biol.* **305**, 131–144 (2012).

18. Lacruz, R. S., Dean, M. C., Ramirez-Rozzi, F. & Bromage, T. G. Megadontia, striae periodicity and patterns of enamel secretion in Plio-Pleistocene fossil hominins. *J. Anat.* **213**, 148–158 (2008).

19. Lacruz, R. S., Habelitz, S., Wright, J. T. & Paine, M. L. Dental enamel formation and implications for oral health and disease. *Physiol. Rev.* **97**, 939–993 (2017).

20. Dean, M. C. Tooth microstructure tracks the pace of human life-history evolution. *Proc. R. Soc. B* **273**, 2799–2808 (2006).

21. Müller, W. & Anczkiewicz, R. Accuracy of laser-ablation (LA)-MC-ICPMS Sr isotope analysis of (bio)apatite-a problem reassessed. *J. Anal. At. Spectrom.* **31**, 259–269 (2016).

22. Müller, W. *et al.* Enamel mineralization and compositional time-resolution in human teeth evaluated via histologically-defined LA-ICPMS profiles. *Geochim. Cosmochim. Acta* **255**, 105–126 (2019).

23. Li, Q. *et al.* Spatially-resolved Ca isotopic and trace element variations in human deciduous teeth record diet and physiological change. *Environ. Archaeol.* 1–10 (2020). doi:10.1080/14614103.2020.1758988

24. Elias, R. W., Hirao, Y. & Patterson, C. C. The circumvention of the natural biopurification of calcium along nutrient pathways by atmospheric inputs of industrial lead. *Geochim. Cosmochim. Acta* **46**, 2561–2580 (1982).

25. Burton, J. H., Price, T. D. & Middleton, W. D. Correlation of bone Ba/Ca and Sr/Ca due to biological purification of Calcium. *J. Archaeol. Sci.* **26**, 609–616 (1999).

26. Balter, V. *et al.* Ecological and physiological variability of Sr/Ca and Ba/Ca in mammals of West European mid-Würmian food webs. *Palaeogeogr. Palaeoclimatol. Palaeoecol.* **186**, 127–143 (2002).

27. Pate, F. D. Bone chemistry and paleodiet. *J. Archaeol. Method Theory* **1**, 161–209 (1994).

28. Kohn, M. J., Morris, J. & Olin, P. Trace element concentrations in teeth - a modern Idaho baseline with implications for archeometry, forensics, and palaeontology. *J. Archaeol. Sci.* **40**, 1689–1699 (2013).

29. de Vos, J. Faunal Stratigraphy and Correlation of the Indonesian Hominid Sites. In *Ancestors: The Hard Evidence* (ed Delson, E.) 215-220 (Alan R. Liss, Inc., New York, 1985).

30. de Vos, J. *et al.* The *Homo* bearing deposits of Java and its ecological context. *Cour. Forsch. Inst. Senckenberg* **171**, 129–140 (1994).

31. Leinders, J. J. M. *et al.* The age of the hominid-bearing deposits of Java: State of the art. *Geol. Mijnbouw* **64**, 167-173 (1985).

32. Sondaar, P. Faunal evolution and the mammalian biostratigraphy of Java. In *The Early Evolution of Man* (eds Andrews, P. & Franzen, J.) *Cour. Forsch. Inst. Senckenberg* **69**, 219-235 (1984).

33. Peek, S. & Clementz, M. T. Sr/Ca and Ba/Ca variations in environmental and biological sources: A survey of marine and terrestrial systems. *Geochim. Cosmochim. Acta* **95**, 36–52 (2012).

34. Reynard, B. & Balter, V. Trace elements and their isotopes in bones and teeth: Diet, environments, diagenesis, and dating of archeological and paleontological samples. *Palaeogeogr. Palaeoclimatol. Palaeoecol.* **416**, 4–16 (2014).

35. Jacques, L. *et al.* Implications of diagenesis for the isotopic analysis of Upper Miocene large mammalian herbivore tooth enamel from Chad. *Palaeogeogr. Palaeoclimatol. Palaeoecol.* **266**, 200-210 (2008).

36. Brumfitt, I. M., Chinsamy, A. & Compton, J. S. Depositional environment and bone diagenesis of the Mio/Pliocene Langebaanweg bonebed, South Africa. *S. Afr. J. Geol.* **116**, 241-258 (2013).

37. Decrée, S. *et al.* The post-mortem history of a bone revealed by its trace element signature: the case of a fossil whale rostrum. *Chem. Geol.* **477**, 137-150 (2018).

38. Janssen, R. *et al.* Tooth enamel stable isotopes of Holocene and Pleistocene fossil fauna reveal glacial and interglacial paleoenvironments of hominins in Indonesia. *Quat. Sci. Rev.* **144**, 145–154 (2016).

39. Blumenthal, S. A. *et al.* Stable isotope time-series in mammalian teeth: In situ $\delta^{18}O$ from the innermost enamel layer. *Geochim. Cosmochim. Acta* **124**, 223–236 (2014).

40. Zazzo, A., Balasse, M. & Patterson, W. P. High-resolution $\delta^{13}C$ intratooth profiles in bovine enamel: Implications for mineralization pattern and isotopic attenuation. *Geochim. Cosmochim. Acta* **69**, 3631–3642 (2005).

41. Deutsch, D. & Pe'er, E. Development of enamel in human fetal teeth. *J. Dent. Res.* **61**, 1543–1551 (1982).

42. Dean, C. *et al.* Growth processes in teeth distinguish modern humans from *Homo erectus* and earlier hominins. *Nature* **414**, 628–631 (2001).

42. Guatelli-Steinberg, D., Ferrell, R. J. & Spence, J. Linear enamel hypoplasia as an indicator of physiological stress in great apes: Reviewing the evidence in light of enamel growth variation. *Am. J. Phys. Anthropol.* **148**, 191–204 (2012).

43. Cerling, T. E. *et al.* Woody cover and hominin environments in the past 6 million years. *Nature* **476**, 51–56 (2011).

44. Lacruz, R. S., Dean, M. C., Ramirez-Rozzi, F. & Bromage, T. G. Megadontia, striae periodicity and patterns of enamel secretion in Plio-Pleistocene fossil hominins. *J. Anat.* **213**, 148–158 (2008).

45. Reid, D. J. & Dean, M. C. Variation in modern human enamel formation times. *J. Hum. Evol.* **50**, 329–346 (2006).

46. Smith, T. M. Dental development in living and fossil orangutans. *J. Hum. Evol.* **94**, 92–105 (2016).

47. Schwartz, G. T., Reid, D. J. & Dean, C. Developmental aspects of sexual dimorphism in hominoid canines. *Int. J. Primatol.* **22**, 837–860 (2001).

493 48. Bonhommeau, S. *et al.* Eating up the world's food web and the human trophic level.
494 *Proc. Natl. Acad. Sci. USA* **110**, 20617–20620 (2013).

495 49. Sponheimer, M. & Lee-Thorp, J. A. Enamel diagenesis at South African australopith
496 sites: Implications for paleoecological reconstruction with trace elements. *Geochim.*
497 *Cosmochim. Acta* **70**, 1644–1654 (2006).

498 50. Eltringham, S. K. The pygmy hippopotamus (*Hexaprotodon liberiensis*). in *Pigs,*
499 *Peccaries and Hippos* (ed Oliver, W.) 55–60 (International Union for the Conservation
500 of Nature and Natural Resources, Gland, 1993).

501 51. Jablonski, N. G. The hippo's tale: How the anatomy and physiology of Late Neogene
502 Hexaprotodon shed light on Late Neogene environmental change. *Quat. Int.* **117**,
503 119–123 (2004).

504 52. Hendier, A. Diet determination of wild pygmy hippopotamus (*Choeropsis liberiensis*).
505 (University of Neuchâtel, Switzerland, 2019).

506 53. Klein, I. Ernährung und ökologisches Profil von *Axis lydekkeri*. (Goethe University
507 Frankfurt, 2020).

508 54. Russon, A. E. *et al.* Geographic variation in orangutan diets. In *Orangutans:*
509 *Geographic variation in behavioral ecology and conservation* (eds Wich, S. A., Suci
510 Utami Atmoko, S., Mitra Setia, T. & van Schaik, C. P.) 135-156 (Oxford University
511 Press, Oxford, 2009).

512 55. Kanamori, T. *et al.* Feeding ecology of Bornean orangutans (*Pongo pygmaeus morio*)
513 in Danum Valley, Sabah, Malaysia: a 3-year record including two mast fruitings. *Am.*
514 *J. Primatol*. **72**, 820–840 (2010).

515 56. Kanamori, T., Kuze, N., Bernard, H., Malim, T. P. & Kohshima, S. Fluctuations of
516 population density in Bornean orangutans (*Pongo pygmaeus morio*) related to fruit

availability in the Danum Valley, Sabah, Malaysia: a 10-year record including two mast fruitings and three other peak fruitings. *Primates* **58**, 225–235 (2017).

57. Sémah, A.-M., Sémah B, F., Djubiantono, T. & Brasseur, B. Landscapes and hominids' environments: Changes between the Lower and the early Middle Pleistocene in Java (Indonesia). *Quat. Int.* **4**, 451 (2009).

58. Sémah, A. M. & Sémah, F. The rain forest in Java through the Quaternary and its relationships with humans (adaptation, exploitation and impact on the forest). *Quat. Int.* **249**, 120–128 (2012).

59. Brasseur, B., Sémah, F., Sémah, A.-M. & Djubiantono, T. Approche paléopédologique de l'environnement des hominidés fossiles du dôme de Sangiran (Java central, Indonésie). *Quaternaire* **22**, 13–34 (2011).

60. Smith, T. M., Austin, C., Hinde, K., Vogel, E. R. & Arora, M. Cyclical nursing patterns in wild orangutans. *Sci. Adv.* **3**, e1601517 (2017). (57)

61. Humphrey, L. T. Isotopic and trace element evidence of dietary transitions in early life. *Ann. Hum. Biol.* **41**, 348–357 (2014).

62. Widdowson, E. M. Absorption, excretion and storage of trace elements: studies over 50 years. *Food Chem.* **43**, 203-207 (1992).

63. Dean, C., Le Cabec, A., Spiers, K., Zhang, Y. & Garrevoet, J. Incremental distribution of strontium and zinc in great ape and fossil hominin cementum using synchrotron X-ray fluorescence mapping. *J. R. Soc. Interface* **15**, (2018).

64. Dean, M. C., Le Cabec, A., Van Malderen, S. J. M. & Garrevoet, J. Synchrotron X-ray fluorescence imaging of strontium incorporated into the enamel and dentine of wild-shot orangutan canine teeth. *Arch. Oral Biol.* **119**, 104879 (2020).

65. Pontzer, H., Raichlen, D. A., Shumaker, R. W., Ocobock, C. & Wich, S. A. Metabolic adaptation for low energy throughput in orangutans. *Proc. Natl. Acad. Sci. USA* **107**, 14048–14052 (2010). (60)

66. Mahaney, W. C., Hancock, R. G. V, Aufreiter, S., Milner, M. W. & Voros, J. Bornean orangutan geophagy: analysis of ingested and control soils. *Environ. Geochem. Health* **38**, 51-64 (2016).

67. Austin, C. *et al.* Uncovering system-specific stress signatures in primate teeth with multimodal imaging. *Scientific Reports* **6**, 1-11 (2016).

68. Humphrey, L. T. Weaning behaviour in human evolution. *Semin. Cell Dev. Biol.* **21**, 453–461 (2010).

69. van Noordwijk, M. A., Willems, E. P., Utami Atmoko, S. S., Kuzawa, C. W. & van Schaik, C. P. Multi-year lactation and its consequences in Bornean orangutans (*Pongo pygmaeus wurmbii*). *Behav. Ecol. Sociobiol.* **67**, 805–814 (2013). (55)

70. Galdikas, B. M. F. & Wood, J. W. Birth spacing patterns in humans and apes. *Am. J. Phys. Anthropol.* **83**, 185–191 (1990).

71. van Noordwijk, M. A. & van Schaik, C. P. Development of ecological competence in Sumatran orangutans. *Am. J. Phys. Anthropol.* **127**, 79–94 (2005).

72. Leuser National Park, G., Sugardjito, J., te Boekhorst, J. A. & van Hooff, J. A. R. A. M. Ecological constraints on the grouping of wild orang-utans (*Pongo pygmaeus*) in the Gunung Leuser National Park, Sumatra, Indonesia. *Int. J. Primatol.* **8**, 17–41 (1987).

73. Wich, S. A. *et al.* Life history of wild Sumatran orangutans (*Pongo abelii*). *J. Hum. Evol.* **47**, 385–398 (2004).

74. Dubois, E. Palaeontologische onderzoekingen op Java. Extra bijvoegsel der Javasche Courant, Verlag van het Mijnwezen over het 3e kwartaal pp. 12–14 (1891).

75. Dubois, E. *Pithecanthropus erectus*, einen menschenaehnliche Uebergangsform aus Java. Landesdruckerei, Batavia (1894).

76. Joordens, J. C. A. *et al. Homo erectus* at Trinil on Java used shells for tool production and engraving. *Nature* **518**, 228–231 (2015).

77. Ungar, P. S., Grine, F. E. & Teaford, M. F. Diet in early *Homo* : A review of the evidence and a new model of adaptive versatility. *Annu. Rev. Anthropol.* **35**, 209–228 (2006).

78. Tausch, J. A New Method for Examining Hominin Dietary Strategy: Occlusal Microwear Vector Analysis of the Sangiran 7 *Homo erectus* Molars. (Goethe University Frankfurt, 2011).

79. Tausch, J., Kullmer, O. & Bromage, T. G. A new method for determining the 3D spatial orientation of molar microwear. *Scanning* **37**, 446–457 (2015).

80. Caropreso, S. *et al.* Thin sections for hard tissue histology: A new procedure. *J. Microsc.* **199**, 244–247 (2000).

81. Bondioli, L., Nava, A., Rossi, P. F., & Sperduti, A. Diet and health in Central-Southern Italy during the Roman Imperial time. *Acta IMEKO* **5**, 19-25 (2016).

82. Müller, W., Shelley, M., Miller, P. & Broude, S. Initial performance metrics of a new custom-designed ArF excimer LA-ICPMS system coupled to a two-volume laser-ablation cell. *J. Anal. At. Spectrom.* **24**, 209–214 (2009).

83. Evans, D. & Müller, W. LA-ICPMS elemental imaging of complex discontinuous carbonates: An example using large benthic foraminifera. *J. Anal. At. Spectrom.* **28**, 1039–1044 (2013).

84. Longerich, H. P., Jackson, S. E. & Günther, D. Laser ablation inductively coupled plasma mass spectrometric transient signal data acquisition and analyte concentration calculation. *J. Anal. At. Spectrom.* **11**, 899–904 (1996).

85. Retief, D. H., Cleaton-Jones, P. E., Turkstra, J. & De Wet, W. J. The quantitative analysis of sixteen elements in normal human enamel and dentine by neutron activation analysis and high-resolution gamma-spectrometry. *Arch. Oral Biol.* **16**, 1257–1267 (1971).

86. Lacruz, R. S. Enamel: Molecular identity of its transepithelial ion transport system. *Cell Calcium* **65**, 1–7 (2017).

87. Klemme, S. *et al.* Synthesis and preliminary characterisation of new silicate, phosphate and titanite reference glasses. *Geostand. Geoanalytical Res.* **32**, 39–54 (2008).

88. Jochum, K. P. *et al.* Accurate trace element analysis of speleothems and biogenic calcium carbonates by LA-ICP-MS. *Chem. Geol.* **318**–**319**, 31–44 (2012).

89. Garbe-Schönberg, D. & Müller, S. Nano-particulate pressed powder tablets for LA-ICP-MS. *J. Anal. At. Spectrom.* **29**, 990–1000 (2014).

90. Jochum, K. P. *et al.* Nano-powdered calcium carbonate reference materials: significant progress for microanalysis? *Geostand. Geoanalytical Res.* **43**, 595–609 (2019).

91. Cleveland, W. S., Grosse, E. & Shyu, W. M. Local regression models. In *Statistical Models in S* (eds Chambers, J. M. & Hastie, T.) 309–376 (Chapman and Hall/CRC, New York, 1992).

92. Guatelli-Steinberg, D., Floyd, B. A., Dean, M. C. & Reid, D. J. Enamel extension rate patterns in modern human teeth: Two approaches designed to establish an integrated comparative context for fossil primates. *J. Hum. Evol.* **63**, 475–486 (2012).

93. Birch, W. & Dean, M. C. A method of calculating human deciduous crown formation times and of estimating the chronological ages of stressful events occurring during deciduous enamel formation. *J. Forensic Leg. Med.* **22**, 127–144 (2014).

94. Spötl, C. & Vennemann, T. W. Continuous-flow isotope ratio mass spectrometric analysis of carbonate minerals. *Rapid Commun. Mass Spectrom.* **17**,1004–1006 (2003).

Acknowledgements

We express our gratitude to the Werner Reimers Foundation in Bad Homburg (Germany), which provides the Gustav Heinrich Ralph von Koenigswald collection as a permanent loan for scientific research to the Senckenberg Research Institute and Natural History Museum Frankfurt. FIERCE, where all LA-ICPMS analyses were performed, is financially supported by the Wilhelm and Else Heraeus Foundation and by the Deutsche Forschungsgemeinschaft (DFG, INST 161/921-1 FUGG and INST 161/923-1 FUGG), which are gratefully acknowledged. We thank Linda Marko and Axel Gerdes for help with analytical work. We thank Rainer Brocke and Gunnar Riedel for assistance with microscopic imaging. C. Z. acknowledges the support of the French CNRS (Centre National de la Recherche Scientifique). J.K. received funding from the Erasmus+ Traineeship program (2019). A. N. received funding from the European Union's Horizon 2020 research and innovation programme under the Marie Skłodowska-Curie grant agreement (No.842812). T.L. received funding from the DFG (Emmy Noether Fellowship LU 2199/2-1). We thank the three journal reviewers (T. Smith and two anonymous) for their helpful comments, which considerably improved both content and clarity of presentation of this paper.

Author contributions

The study was initiated by W M., F. S. and J. K. and forms part of J. K.'s MSc research project completed under the supervision of W. M., L. B. and A. N. J. K., W. M., A. N., L. B., F. S. and O. K. designed research, J. K., W. M., A. N., L. B., B. P., T. L. and R. A. performed research, J. K., W. M., A. N., T. L. and L. B. analyzed data, J. K., W. M., A. N., L. B., F. S., O. K., C. Z., T. L. and C. H. wrote the manuscript with contributions from all other authors.

Data availability

The raw data of element analyses used in this study are available as a separate Excel file.

Competing interests

The authors declare no competing interests.

Additional Information

Supplementary information is available in the online version of the paper.

Reprints and permissions information is available at www.nature.com/reprints.

Correspondence and requests for materials should be addressed to J. K. (juelide.kubat@gmail.com), A. N. (alessianava@gmail.com) and W.M. (w.muller@em.uni-frankfurt.de).

Table 1 | List of specimens from the GHR v. Koenigswald Collection used in the present study. The specimens are housed in the Department of Palaeoanthropology, Senckenberg Research Institute and Natural History Museum Frankfurt, Frankfurt a. M., Germany.

	Catalogue number	**Taxonomic identification**	**Dental elements**
PRIMATES	S7-13	Hominidae/*Homo erectus*	upper left M
	S7-37	Hominidae/*Homo erectus*	right P^4
	SMF-8865	Hominidae/*Homo erectus*	lower left M
	SMF-8864	Hominidae/*Pongo* sp.	lower right M
CARNIVORA	SMF/PA/F6664	Felidae/*Panthera tigris*	right P_4
	SMF/PA/F6666	Felidae/*Panthera tigris*	right M_1
PERISSODACTYLA	SMF/PA/F5941	Rhinoceratidae/ *Rhinoceros sondaicus*	left M_1
	SMF/PA/F5950	Rhinoceratidae/ *Rhinoceros sondaicus*	left M_2
ARTIODACTYLA	SMF/PA/F738	Suidae/*Sus* sp.	right M^3
	SMF/PA/F869	Suidae/*Sus* sp.	right M^3
	SMF/PA/F5077	Cervidae/*Axis lydekkeri*	left M_2
	SMF/PA/F5258	Cervidae/*Axis lydekkeri*	right P^3, M^1, M^2, M^3
	SMF/PA/F6	Hippopotamidae/ *Hexaprotodon* sp.	right M^2
	SMF/PA/F53	Hippopotamidae/ *Hexaprotodon* sp.	left M_2

Table 2 | Track lengths and Retzius Periodicity of the hominid sample.

Catalogue number	Taxon	Tooth type	Cusp/aspect	Track lenght [µm]	Track length [years]	Retzius Periodicity [days]
S7-13	*Homo erectus*	upper left M	paracone/buccal	4303	1.9	7 or 8*
S7-13	*Homo erectus*	upper left M	protocone/palatal	3629	1.8	
S7-37	*Homo erectus*	right P^4	protocone/palatal	6470	2.9[+]	7***
SMF-8865	*Homo erectus*	lower left M	protoconid/buccal	6252	3.1	8 or 9*
SMF-8865	*Homo erectus*	lower left M	metaconid/lingual	3906	-****	
SMF-8864	*Pongo* sp.	lower right M	protoconid/buccal	6009	2.9	8***
SMF-8864	*Pongo* sp.	lower right M	metaconid/lingual	5660	3.7	

*based on local DSRs between adjacent Retzius lines and not direct counts of cross striations due to section thickness; ** reported in Lacruz et al 2008[18] for S7-37 M^1; ***direct counts of cross striations; ****section plane off centre, cervical portion damaged; [+]Track length in years derived from the revised crown formation time, which is slightly longer than reported in Lacruz et al. 2008[18].

673 Fig. 1 | Scatter plots of [Sr] or [Ba] vs. [Mn], respectively, for representative examples of each faunal
674 group, to illustrate the diagenesis assessment of the fossil assemblage. See Supplementary Figure
675 1 for equivalent plots relative to [U]. For simplicity, data are here shown as concentrations, whereas
676 elsewhere they are displayed as El/Ca to facilitate comparison.
677
678 Fig. 2 | Sr/Ca ratios. Box plot comparing *H. erectus* and *Pongo* sp. specimens to other taxa with
679 known trophic levels, all displayed after diagenesis filtering, i.e. [U]<1 ppm and [Mn]<400 ppm (µg/g)
680 (see Supplementary Fig. 7). Colour dots outside the whiskers represent outliers, lower whisker are
681 equal to minimum value (excluding outliers), lower hinge equals to first quartile, thick line represents
682 the median value, upper hinge equals to third quartile and upper whisker to maximum value
683 (excluding outliers).
684
685 Fig. 3 | Time-resolved compositional profiles for *Pongo* sp. SMF-8864 molar. a) Sr/Ca, Ba/Ca, [U]
686 and [Mn] along the EDJ plotted against relative days. Apart from isolated [U] peaks, only minor
687 diagenetic overprint is discernible for thin enamel from ~925 days. b) Comparative Sr/Ca, [U] and
688 [Mn] profiles along EDJ vs. corresponding prism orientations (Supplementary Fig. 4), plotted against
689 relative days; while data agree well overall, towards outer enamel the latter show lower Sr/Ca values
690 relative to corresponding EDJ positions due to maturation overprint. c) Elemental profiles for both
691 mesiolingual and mesiobuccal cusp showcase the remarkable similarity of Sr/Ca on both enamel
692 sides. Accentuated lines (A. L.) and hypoplastic defects are highlighted. See text for details.
693
694 Fig. 4 | Time-resolved compositional EDJ profiles for all investigated *H. erectus* specimens plotted
695 against their individual relative dental chronologies except for S7-37 where P^4 where
696 odontochronology in life time is known[18]. a) SMF-8865. b) S7-13. c) S7-37. See text for details.
697
698 Fig. 5 | Carbon and oxygen isotope data of enamel from *H. erectus* S7-37 P^4 plotted against life time
699 in relative days and years. Length of coloured bars indicate possible formation times of enamel used
700 for analyses, and thickness indicates 1sd of isotope data (0.03 ‰ for $\delta^{13}C$ and 0.05 ‰ for $\delta^{18}O$,
701 respectively).

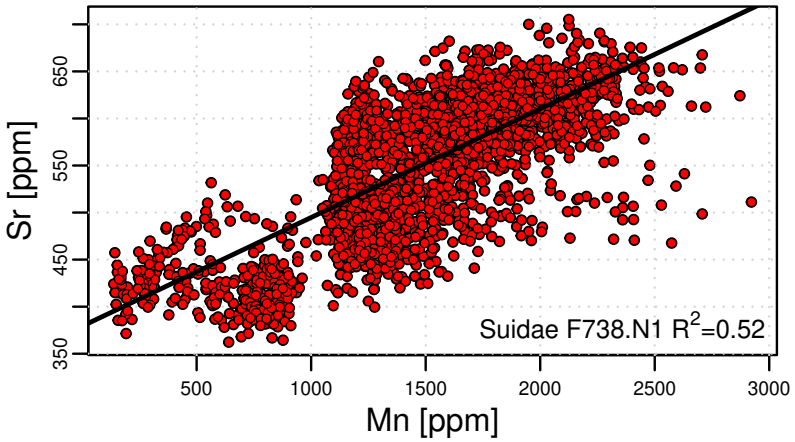
Sr [ppm]
Mn [ppm]
Suidae F738.N1 R2=0.52

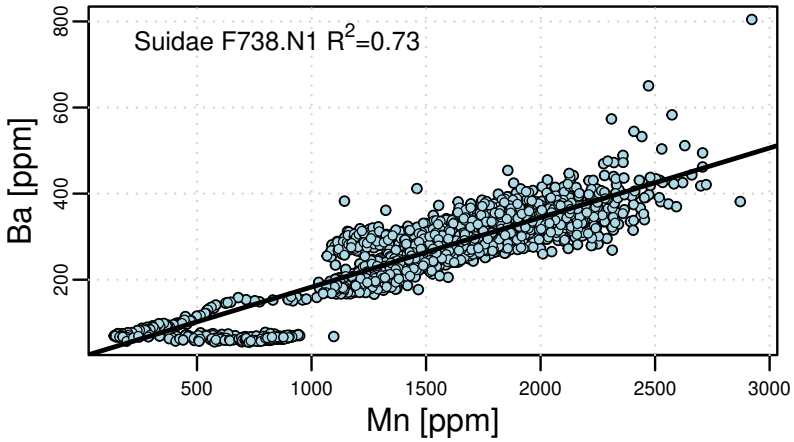
Ba [ppm]
Mn [ppm]
Suidae F738.N1 R2=0.73

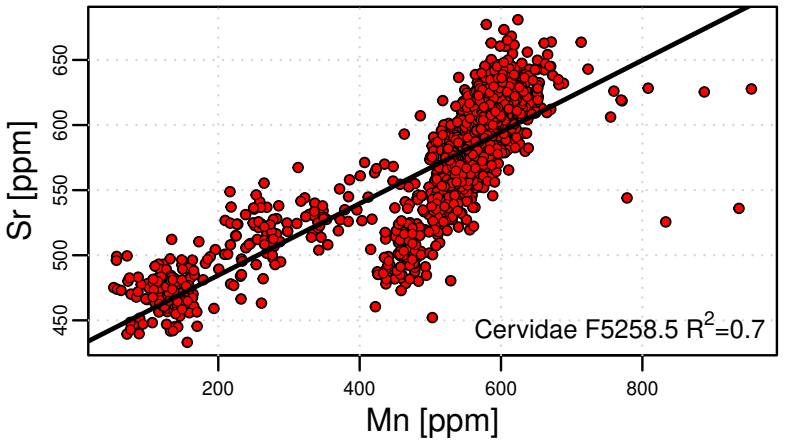
Sr [ppm]
Mn [ppm]
Cervidae F5258.5 R2=0.7

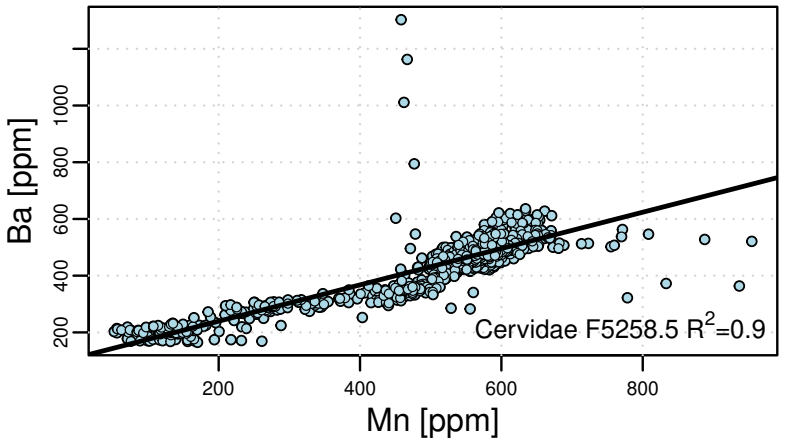
Ba [ppm]
Mn [ppm]
Cervidae F5258.5 R2=0.9

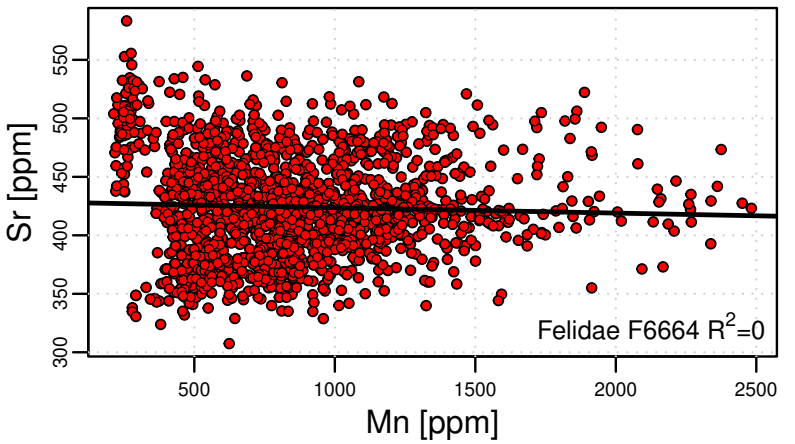
Sr [ppm]
Mn [ppm]
Felidae F6664 R2=0

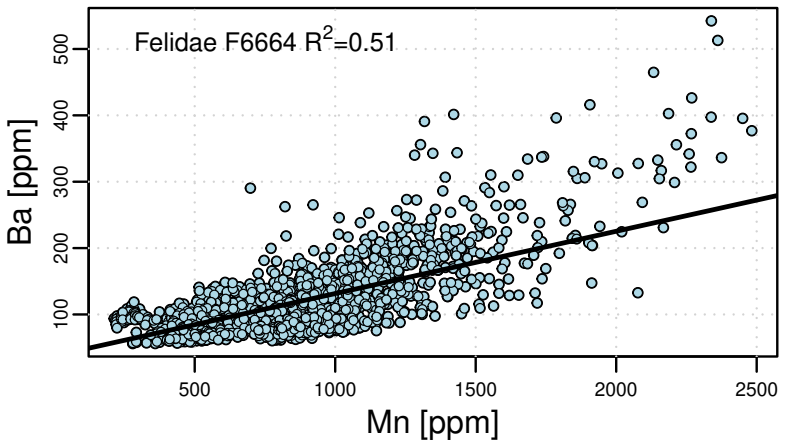
Ba [ppm]
Mn [ppm]
Felidae F6664 R2=0.51

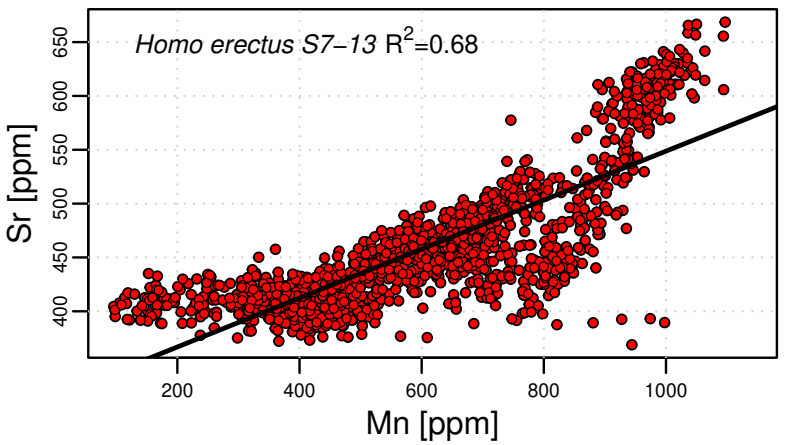
Sr [ppm]
Mn [ppm]
Homo erectus S7–13 R2=0.68

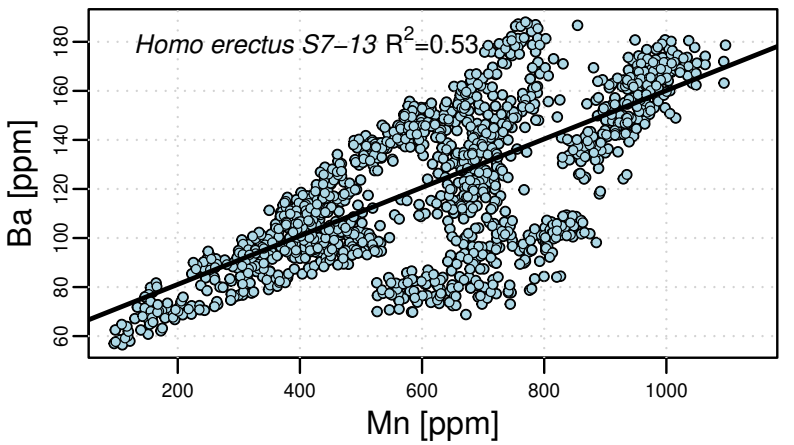
Ba [ppm]
Mn [ppm]
Homo erectus S7–13 R2=0.53

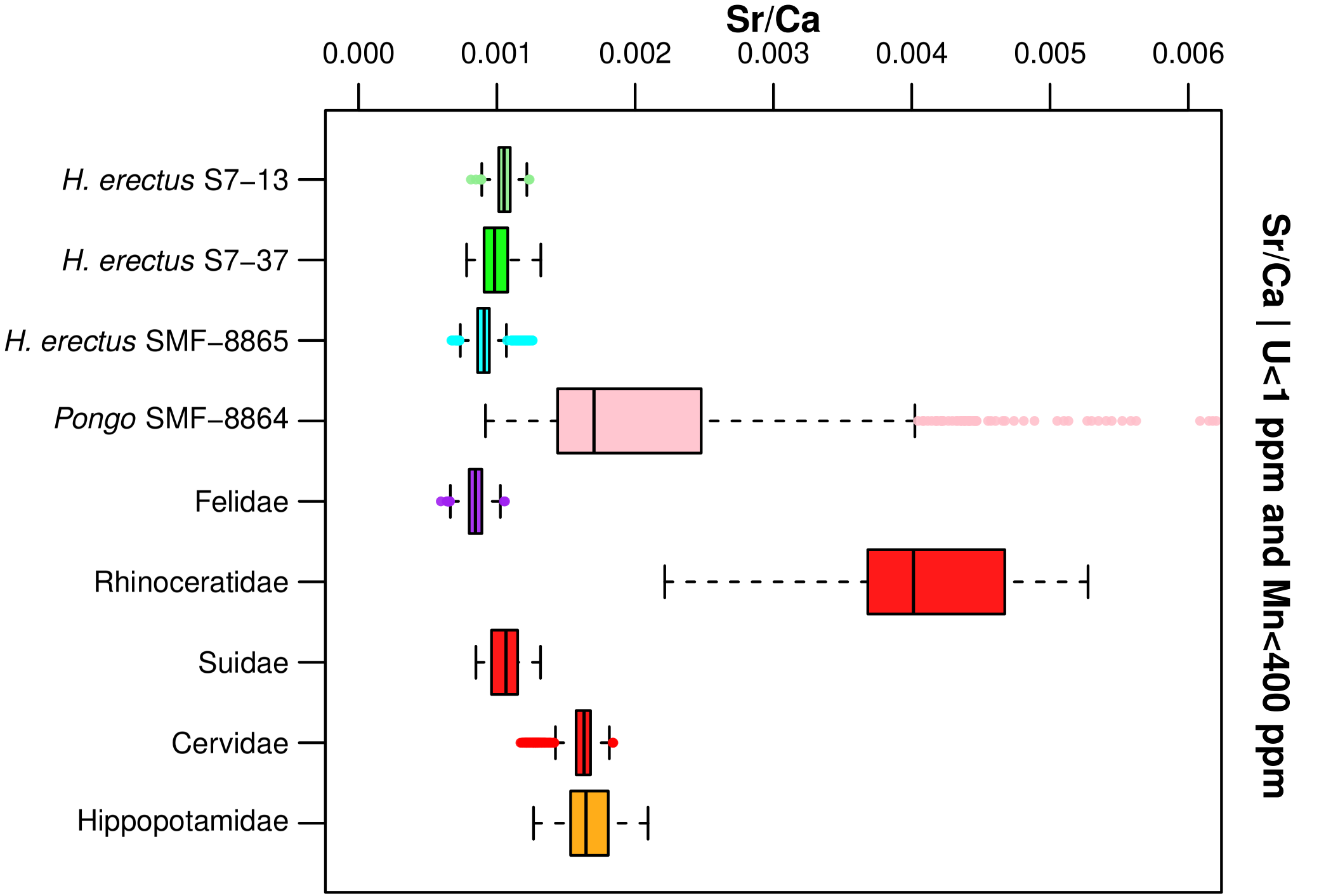
Sr/Ca
0.000
0.001
0.002
0.003
0.004
0.005
0.006
H. erectus S7–13
H. erectus S7–37
H. erectus SMF–8865
Pongo SMF–8864
Felidae
Rhinoceratidae
Suidae
Cervidae
Hippopotamidae
Sr/Ca | U<1 ppm and Mn<400 ppm

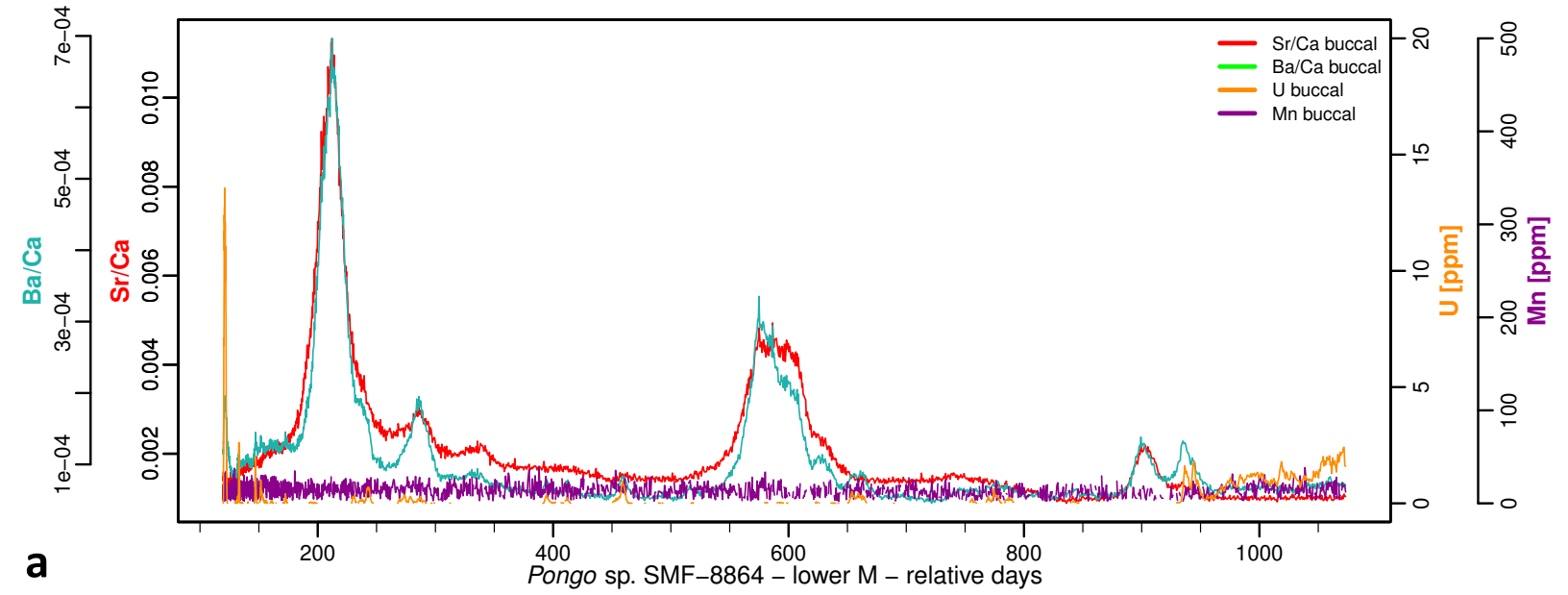
Ba/Ca
Sr/Ca
U [ppm]
Mn [ppm]
Sr/Ca buccal
Ba/Ca buccal
U buccal
Mn buccal
200
400
600
800
1000
Pongo sp. SMF–8864 – lower M – relative days

a

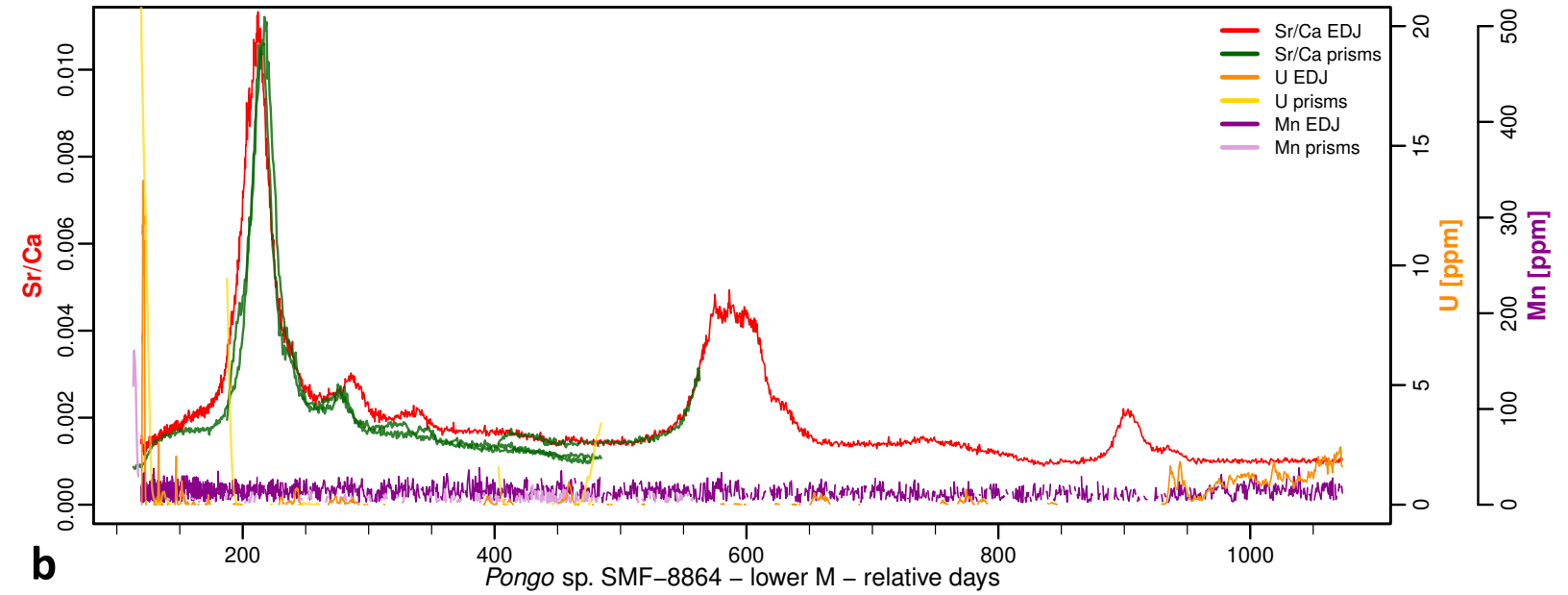
Sr/Ca
U [ppm]
Mn [ppm]
Sr/Ca EDJ
Sr/Ca prisms
U EDJ
U prisms
Mn EDJ
Mn prisms
200
400
600
800
1000
Pongo sp. SMF–8864 – lower M – relative days

b

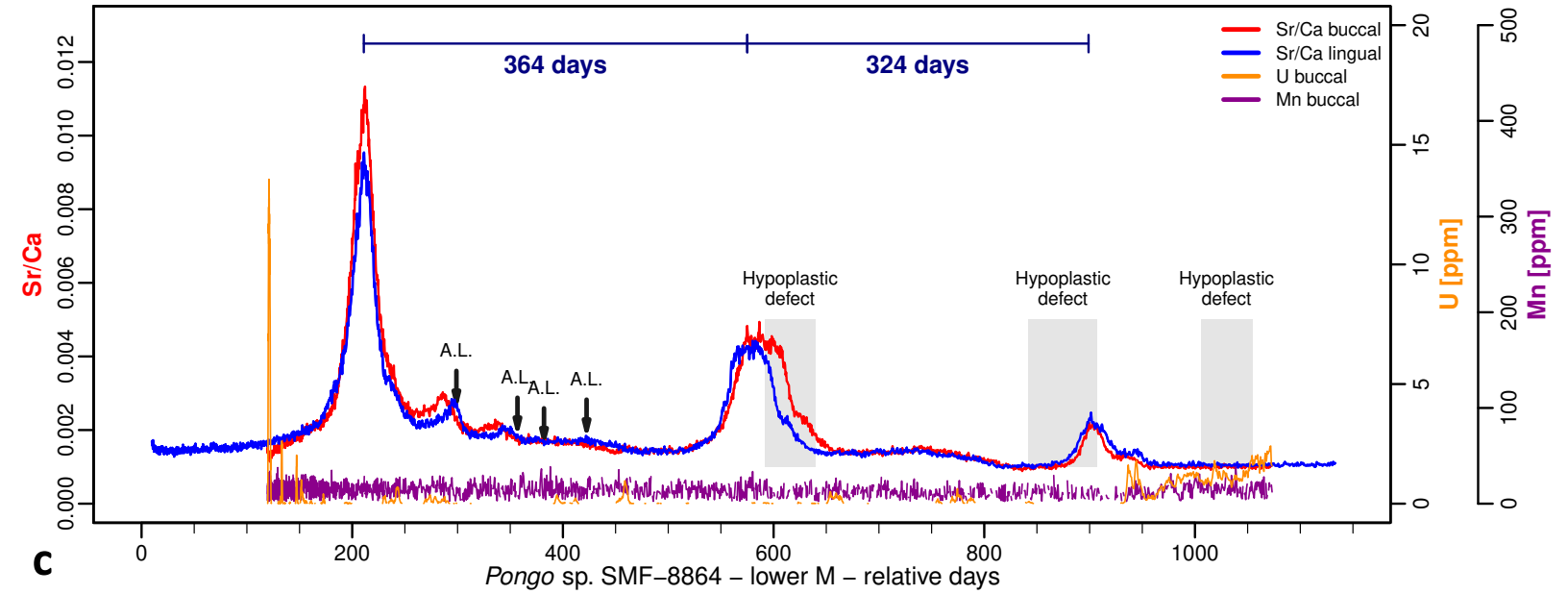
364 days
324 days
Sr/Ca
U [ppm]
Mn [ppm]
Sr/Ca buccal
Sr/Ca lingual
U buccal
Mn buccal
A.L.
A.L.
A.L.
A.L.
Hypoplastic defect
Hypoplastic defect
Hypoplastic defect
0
200
400
600
800
1000
Pongo sp. SMF–8864 – lower M – relative days

c

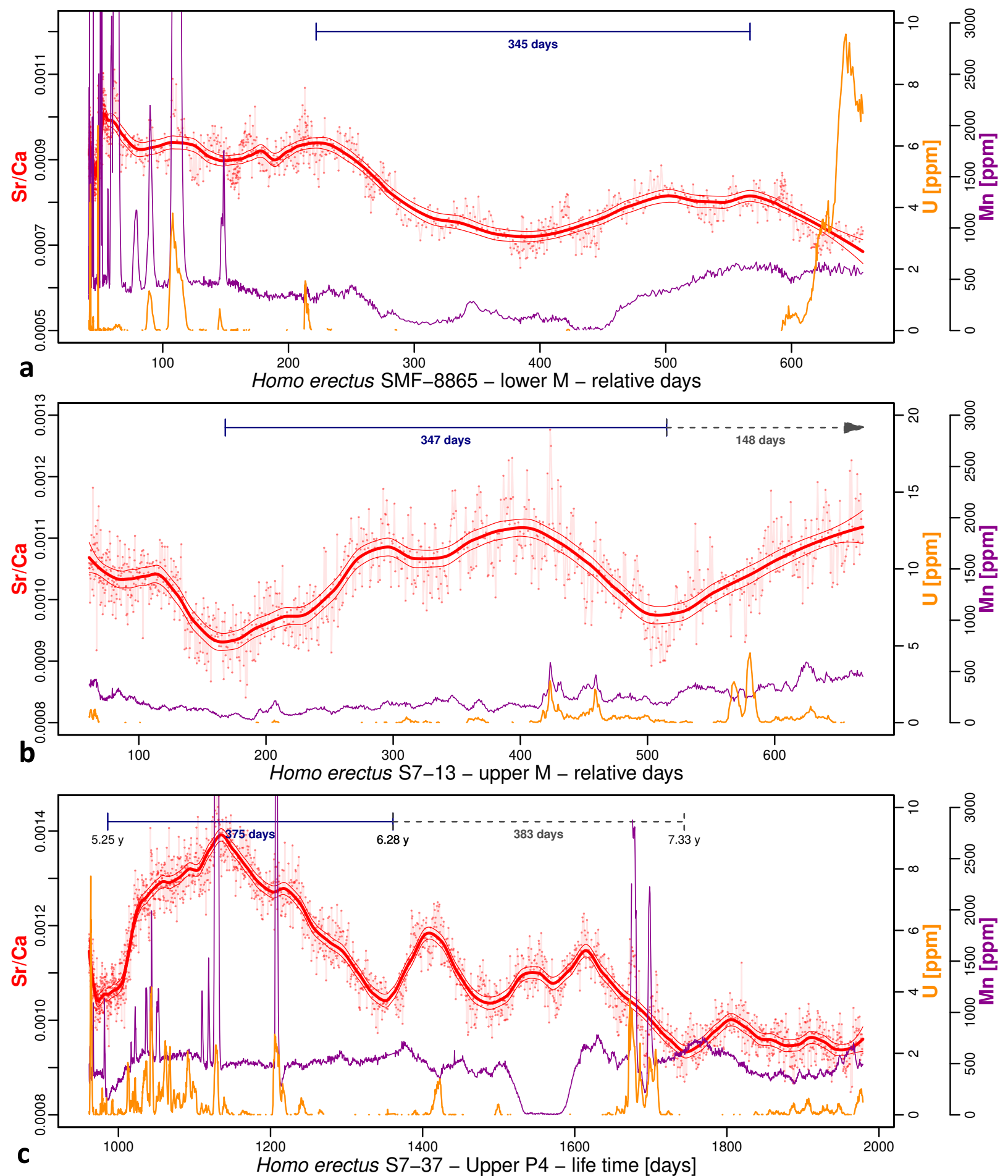
345 days
Sr/Ca
U [ppm]
Mn [ppm]
a
Homo erectus SMF–8865 – lower M – relative days
347 days
148 days
b
Homo erectus S7–13 – upper M – relative days
5.25 y
375 days
6.28 y
383 days
7.33 y
c
Homo erectus S7–37 – Upper P4 – life time [days]

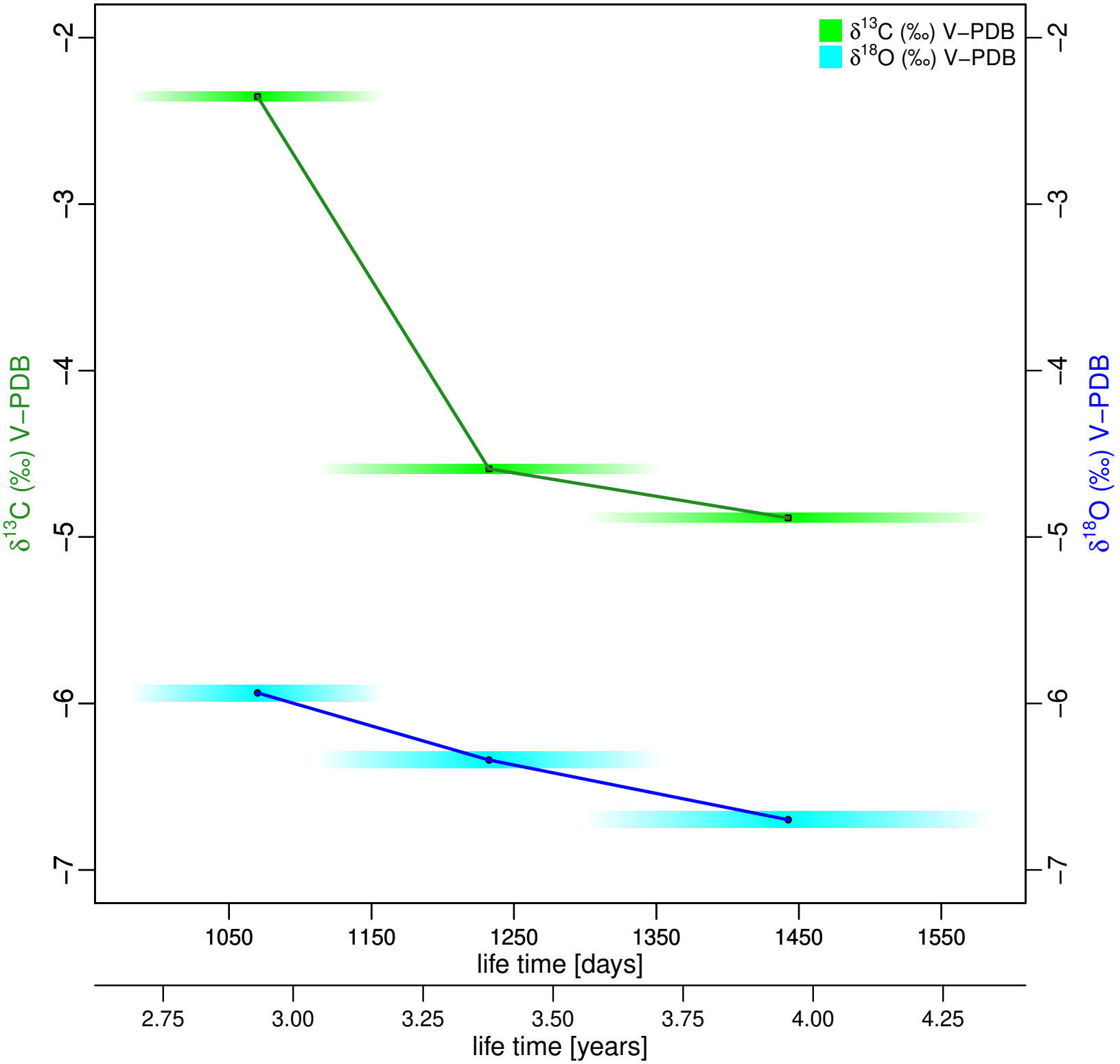
δ13C (‰) V–PDB
δ18O (‰) V–PDB
δ13C (‰) V–PDB
δ18O (‰) V–PDB
−2
−3
−4
−5
−6
−7
1050
1150
1250
1350
1450
1550
life time [days]
2.75
3.00
3.25
3.50
3.75
4.00
4.25
life time [years]